DOI: 10.1002/ejoc.200800567

Molecular Recognition Properties of a Charge-Transfer Host System Composed of 10,10′-Dihydroxy-9,9′-biphenanthryl and Viologen Derivatives

Yoshitane Imai,*[a] Kensaku Kamon,[a] Shingo Kido,[a] Tomohiro Sato,[b] Nobuo Tajima,[c] Reiko Kuroda,[b,d] and Yoshio Matsubara*[a]

Keywords: Charge-transfer complex / Biphenanthryl / Host–guest systems / Molecular recognition / Viologen

A charge-transfer (CT) complex composed of racemic *rac*-10,10′-dihydroxy-9,9′-biphenanthryl as the electron-donor and the diquaternary derivative of 4,4′-bipyridinium (viologen) as the electron-acceptor has been formed by the inclusion of guest molecules. The color and diffuse reflectance spectra of this inclusion CT complex are sensitive to the guest molecules, and their properties can be tuned by changing the component viologen derivatives.

Introduction

The properties of organic compounds in the solid state are different from those in the solution state because in the solid state, molecules are densely packed under the strong influence of the neighboring molecules. In the field of host–guest chemistry, the development of a solid-state molecular recognition system has tremendous potential for the development of novel molecular recognition properties, which would be impossible in the solution state. To date, although several solid-state host systems including organic host molecules have been reported for molecular recognition, they are mostly composed of a single organic molecule.[1] If a solid-state host system is composed of two or more organic molecules, its functionality is enhanced due to the synergistic effect of packing and the properties of the component molecules in the solid state.[2] Recently there has been an increased demand for enhancing the functionalities of these host systems. We have previously developed charge-transfer (CT) host systems composed of 1,1′-bi-2-naphthol derivatives as electron-donors and *p*-benzoquinone or 1,1′-dimethyl-4,4′-bipyridinium dichloride (methylviologen, $MVCl_2$) as electron-acceptors; these host systems serve as excellent visual indicators for guest aromatic molecules.[3] Moreover, by using racemic *rac*-10,10′-dihydroxy-9,9′-biphenanthryl (*rac*-**1**), which with two phenanthrene rings is larger and has more extensive π conjugation, as the electron-donor, a CT host system that includes guest *n*-alkyl alcohol molecules is successfully formed.[4]

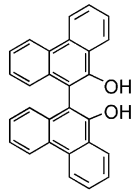

rac-**1**

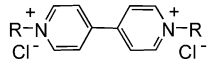

$MVCl_2$: R = Me
$PVCl_2$: R = Ph
$BVCl_2$: R = $PhCH_2$

One of the key properties of these supramolecular host systems is the ability to easily tune the physical and chemical properties of the complex by simply changing the component molecules without involving new synthetic methods. In this paper, we report the molecular recognition behavior and inclusion mechanism of the biphenanthryl CT host system by changing the diquaternary derivatives of 4,4′-bipyridinium (viologen derivatives), which acts as an electron-acceptor. It is inferred that this information is useful for the development of novel solid-state visual indicators for molecular recognition. Three types of viologen derivatives, $MVCl_2$, 1,1′-diphenyl-4,4′-bipyridinium dichloride ($PVCl_2$), and 1,1′-dibenzyl-4,4′-bipyridinium dichloride ($BVCl_2$), were used. Two *n*-alkyl alcohols [*n*-propanol (*n*PrOH) and *n*-butanol (*n*BuOH)] with different chain lengths were used as the guest molecules to study the influence of the size of the included guest molecule on this system.

Results and Discussion

The guest inclusion behavior of the *rac*-**1**/$MVCl_2$ host system was first studied. *rac*-**1** was synthesized by a previously reported method.[5] The inclusion of *n*PrOH or

[a] Department of Applied Chemistry, Faculty of Science and Engineering, Kinki University,
3-4-1 Kowakae, Higashi-Osaka, Osaka 577-8502, Japan
Fax: +81-6-6727-2024
E-mail: y-imai@apch.kindai.ac.jp
y-matsu@apch.kindai.ac.jp
[b] JST ERATO-SORST Kuroda Chiromorphology Team,
4-7-6 Komaba, Meguro-ku, Tokyo 153-0041, Japan
[c] First-Principles Simulation Group, Computational Materials Science Center, NIMS,
Sengen, Tsukuba, Ibaraki 305-0047, Japan
[d] Department of Life Sciences, Graduate School of Arts and Sciences, The University of Tokyo,
3-8-1 Komaba, Meguro-ku, Tokyo 153-8902, Japan

*n*BuOH was attempted by crystallization from the respective alcohol solutions containing *rac*-**1** and $MVCl_2$. As a result, colored inclusion CT crystals **I** and **II** were obtained from *n*PrOH and *n*BuOH solutions, respectively.

Interestingly, the colors of these inclusion CT crystals change with the included guest molecule, that is, the inclusion crystals **I** containing *n*PrOH are red in color, whereas crystals **II** containing *n*BuOH are blue-black. The colors of both these crystals are unique to the solid state as highly concentrated solutions of these crystals are a light-yellow color. The diffuse reflectance spectra (DRS) of **I** and **II** are shown in Figure 1.

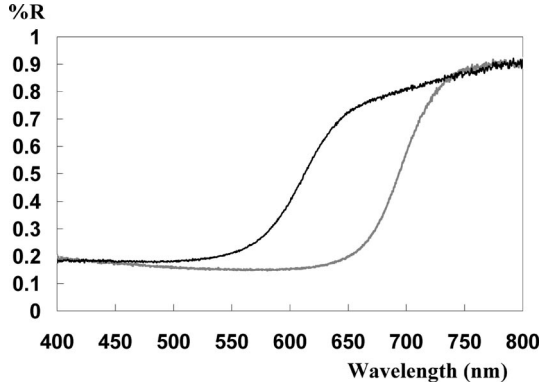

Figure 1. DRS of **I** (black line) and **II** (gray line).

The solid-state DRS of **I** and **II** are also substantially different. The absorption edges of **I** and **II** are located at around 510 and 620 nm, respectively. These results suggest that this *rac*-**1**/$MVCl_2$ host system can function as a visual indicator host system and as an indicator host system in the solid state using DRS.

X-ray analyses of these CT crystals were performed to understand their guest inclusion mechanisms and the origins of their different electronic absorptions. The structure of **I** with the inclusion of *n*PrOH is shown in Figure 2.

The stoichiometry of **I** is (*R*)-**1**/(*S*)-**1**/$MVCl_2$/*n*PrOH/H_2O = 0.5:0.5:0.5:1:1, and the space group is $P\bar{1}$. The (*R*)- and (*S*)-**1** molecules are connected by water molecules through hydrogen-bonding and by chloride ions to form a 1D structural unit (Figure 2, a). The guest *n*PrOH molecules link the hydroxy groups of **1** to the water molecules through hydrogen-bonding; thus, they contribute to the maintenance of the 1D structural unit. Characteristically, cavities (Figure 2, b, indicated by a solid circle) are formed by the self-assembly of this 1D structural unit (Figure 2, b, indicated by a dotted circle) through CT interactions between two 1D structural units and the methylviologen ion (MV^{2+}) (Figure 2, b). These cavities are also maintained by phenanthrene–phenanthrene edge-to-face interactions between the 2-CH unit of one phenanthrene ring and the face of another. In one cavity, two *n*PrOH molecules (Figure 2, b, indicated by a spacefill view) are included. The structure of **II** with the inclusion of *n*BuOH is shown in Figure 3.

Although the stoichiometry of **II** is the same as that of **I**, that is, (*R*)-**1**/(*S*)-**1**/$MVCl_2$/*n*BuOH/H_2O = 0.5:0.5:0.5:1:1, with the same space group $P\bar{1}$, its crystal structure is significantly different. Characteristically, this crystal is composed of a biphenanthrol cluster formed from (*R*)- and (*S*)-**1** molecules connected by hydrogen bonds between a hydroxy group of **1**, two chloride ions, and two water molecules (Figure 3, a). Although the guest *n*BuOH molecules are observed to be disordered, *n*BuOH is clearly linked to a hydroxy group of **1** and a water molecule through hydrogen-bonding and contributes to the maintenance of the biphenanthrol cluster (Figure 3, a). The channel-like cavity along

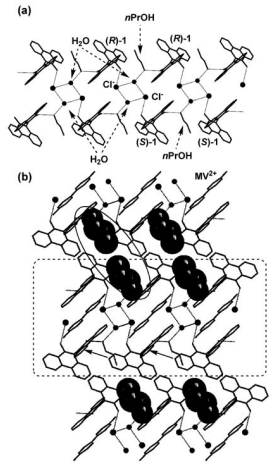

Figure 2. The structure of **I**. (a) Structure of the extracted 1D structure unit. (b) Cavity formed by self-assembly of the 1D structure unit observed along the *a* axis. Solid arrows show phenanthrene–phenanthrene edge-to-face interactions. Dotted circle shows a 1D structure unit. Solid circle shows a cavity.

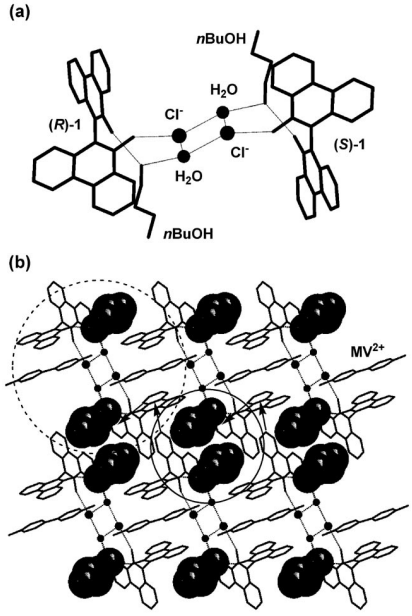

Figure 3. The structure of **II**. (a) Structure of the extracted biphenanthrol cluster. (b) Channel-like cavity formed by self-assembly of the biphenanthrol cluster observed along the *a* axis. Solid arrows show phenanthrene–phenanthrene edge-to-face interactions. Dotted circle shows a biphenanthrol cluster. Solid circle shows a channel-like cavity.

the *a* axis (Figure 3, b, indicated by a solid circle) is formed by the self-assembly of these clusters (Figure 3, b, indicated by a dotted circle) due to CT interactions with MV^{2+} (Figure 3, b). The guest *n*BuOH molecules (Figure 3, b, indicated by the spacefill view) are incorporated into the channel-like cavity. These cavities are also maintained by two types of phenanthrene–phenanthrene edge-to-face interactions (Figure 3, b, indicated by solid arrows), one between the 6-CH of one phenanthrene ring and the face of another (2.95 Å) and the other between the 1-CH of one phenanthrene ring and the face of another (2.94 Å).

The DRS in Figure 1 shows that the difference in the absorptions of **I** and **II** result from the CT absorption bands around the absorption edge. To understand the structural differences leading to these spectra, the intermolecular distances in the X-ray structures were examined (Table 1).

Table 1. Distances between the nearest molecular pairs in **I** and **II**.[a]

	Distance [Å]				
	$MV^{2+}\cdots MV^{2+}$	$MV^{2+}\cdots Cl^-$	$MV^{2+}\cdots$**1**	**1**$\cdots Cl^-$	**1**$\cdots$**1**
I	5.54 (C···C)	3.62 (C···Cl)	3.17 (C···O)	3.10 (O···Cl)	3.33 (C···C)
	6.67 (C···C)	3.56 (C···Cl)	3.37 (C···C)	3.79 (C···Cl)	3.59 (C···O)
II	3.96 (C···C)	3.64 (C···Cl)	3.03 (C···O)	3.11 (O···Cl)	3.49 (C···C)
	6.38 (C···C)	3.67 (C···Cl)	3.21 (C···C)	4.06 (C···Cl)	3.58 (C···O)

[a] The distance between the nearest intermolecular atom pair (non-hydrogen) is provided.

The above data indicates that the major difference between **I** and **II** is in the distance of the nearest $MV^{2+}\cdots MV^{2+}$ pair. The distances between the other molecular pairs are not markedly different, although the global packings of the molecules in these crystals are significantly different, as described above. In both the crystals, the MV cations are dipositive (MV^{2+}) in the ground electronic states, whereas one of the MV cations is monopositive (MV^{+}) in the lowest-energy CT excited states. Thus, a smaller MV···MV distance implies smaller excitation energies because in the excited states an $MV^{+}\cdots MV^{2+}$ interaction occurs, in contrast to the $MV^{2+}\cdots MV^{2+}$ interaction in the ground state. This is most likely one of the factors that leads to the different colors of **I** and **II**.

Next, to tune the molecular recognition properties of this CT host system, the component viologen derivative was changed from $MVCl_2$ to $PVCl_2$. However, *n*PrOH and *n*BuOH were retained as the potential guest molecules, as in the *rac*-**1**/$MVCl_2$ host system. The inclusion of *n*PrOH or *n*BuOH molecules was attempted by crystallization from the corresponding alcohol solutions containing *rac*-**1** and $PVCl_2$ in a manner similar to that described for the *rac*-**1**/$MVCl_2$ host system. However, no inclusion CT crystal was obtained from either of these solutions. In other words, the *rac*-**1**/$PVCl_2$ host system does not include the *n*PrOH or *n*BuOH molecules as guests.

Then, the molecular recognition properties of the *rac*-**1**/$BVCl_2$ host system were studied. The inclusion of *n*PrOH or *n*BuOH was attempted by the same crystallization method from the corresponding alcohol solutions containing *rac*-**1** and $BVCl_2$. In contrast to the *rac*-**1**/$PVCl_2$ host system, colored inclusion CT crystals **III** and **IV** were obtained from the *n*PrOH and *n*BuOH solutions, respectively. Although the colors of **III** and **IV** were also significantly different from those of the component solids, they were a similar red color. Subsequently, the DRS of these crystals were measured and are shown in Figure 4. As expected, the DRS of these CT complexes changed with the included guest alcohol. The absorption edges of **III** and **IV** were located at around 560 and 580 nm, respectively. This shows that this *rac*-**1**/$BVCl_2$ host system can function as an indicator host system in the solid state using DRS. Moreover, these results suggest that the molecular recognition properties of this CT host system can be tuned by changing the viologen derivatives.

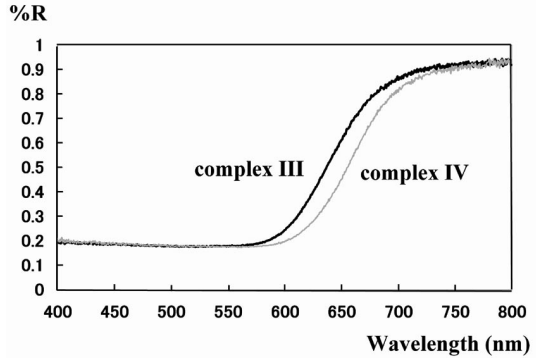

Figure 4. DRS of **III** (black line) and **IV** (gray line).

To understand the guest inclusion mechanisms and the origins of the different electronic absorptions of these CT crystals, X-ray analyses of these crystals were performed. The structure of **III** with the inclusion of *n*PrOH is shown in Figure 5. The stoichiometry of **III** is (*R*)-**1**/(*S*)-**1**/$BVCl_2$/*n*PrOH = 1:1:1:4, and its space group is $P\bar{1}$. The structure of **III** is different to that of **I** and **II**. This crystal has four independent guest *n*PrOH molecules. However, because one of the four *n*PrOH molecules is disordered, this crystal has two types of coordination patterns depending on the disordered *n*PrOH molecule. In one coordination pattern, two types of biphenanthrol clusters (**III-c1** and **III-c2**) are formed from the (*R*)- and (*S*)-**1** molecules connected by hydrogen-bonding between a hydroxy group of **1** and two chloride ions (Figure 5, a and b, respectively). These two biphenanthrol clusters result from differences in the torsion angles of **1**. The torsion angles of **1** in **III-c1** and **III-c2** are 82.9 and 85.4°, respectively. In both clusters, the four guest *n*PrOH molecules are linked. Two of the four *n*PrOH molecules link the hydroxy group of **1** and a chloride ion through hydrogen-bonding and contribute to the maintenance of the biphenanthrol cluster. The other two *n*PrOH molecules link a chloride ion through a hydrogen bond. On the other hand, in the other coordination pattern, the (*R*)-

and (*S*)-**1** molecules are connected through chloride ions by hydrogen-bonding to form a 1D structural unit without water molecules (Figure 5, c). Two of the four *n*PrOH molecules are linked to the hydroxy group of **1** and chloride ions through hydrogen-bonding and contribute to the maintenance of the 1D structural unit. The other two *n*PrOH molecules are linked to a chloride ion through hydrogen-bonding. These guest *n*PrOH molecules (Figure 5, d, indicated by a spacefill view) are incorporated into the cavity formed by the self-assembly of these two clusters and the 1D structural unit by CT interactions with the benzylviologen ion (BV^{2+}). These cavities are also maintained by two phenanthrene–phenanthrene edge-to-face interactions (Figure 5, d, indicated by solid arrows, 2.76 and 2.86 Å, respectively) between the 7-CH of one phenanthrene ring and the face of another phenanthrene ring.

The structure of **IV** with the inclusion of *n*BuOH is shown in Figure 6. The stoichiometry of **IV** is (*R*)-**1**/(*S*)-**1**/$BVCl_2$/*n*BuOH = 1:1:1:2, with the same space group of $P\bar{1}$ as in the case of **III**. The structure of **IV** is different to that of **I**, **II**, and **III**. The crystal of **IV** is composed of two types of biphenanthrol component units (**IV-c1** and **IV-c2**). **IV-c1** is composed of one biphenanthrol unit and a guest *n*BuOH molecule linked to a chloride ion through hydrogen-bonding (Figure 6, a). **IV-c2** is a biphenanthrol cluster formed from the (*R*)- and (*S*)-**1** molecules connected by hydrogen bonds between the hydroxy groups of **1** and two chloride ions (Figure 6, b). The guest *n*BuOH molecule is linked to a hydroxy group of **1** and a chloride ion through hydrogen-bonding and contributes to the maintenance of **IV-c2** (Figure 6, b). Characteristically, a channel-like cavity along the *a* axis is formed by the self-assembly of four **IV-c1** units (Figure 6, c, indicated by a dotted circle) and two **IV-c2** component units (Figure 6c, indicated by a solid circle) through CT interactions with BV^{2+} (Figure 6, c). These cavities are maintained by six phenanthrene–phenanthrene edge-to-face interactions (Figure 6, c, indicated by solid arrows, 2.62 Å for 2-CH, 2.71 Å for 6-CH, 2.72 Å for 3-CH, 2.72 Å for 4-CH, 2.73 Å for 1-CH, 2.81 Å for 6-CH, and 2.83 Å for 1-CH) between the CH of one phenanthrene ring and the face of another. The guest *n*BuOH molecules (Figure 6, c, indicated by a space-fill view) are incorporated into the channel-like cavities. The X-ray crystallographic analyses suggest that this CT host system includes different *n*-alkyl alcohols by changing the combination and coordination pattern of **1**, the chloride ion, and the water molecule.

As in the case of the *rac*-**1**/$MVCl_2$ host system, the intermolecular distances of **III** and **IV** have been examined by X-ray analysis (Table 2). In this case, the main difference between **III** and **IV** lies in the distance between the nearest viologen-cation···viologen-cation pair; the distances between the other molecule pairs are not markedly different, although the global packings of the molecules in these crystals are different, as described above. The $BV^{2+}\cdots BV^{2+}$ distance in **IV** is smaller than in **III**, and this results in smaller energy absorptions in the former than in the latter.

A comparison of the *rac*-**1**/$MVCl_2$ and *rac*-**1**/$BVCl_2$ host systems shows that the colors and DRS of the *n*BuOH com-

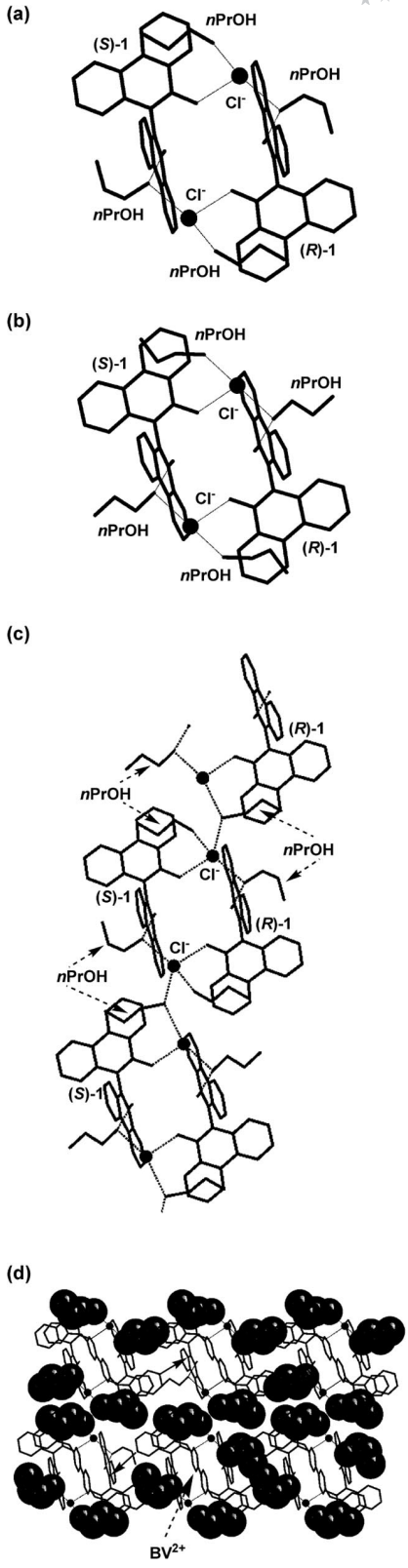

Figure 5. Structure of **III**. (a) Structure of the extracted biphenanthrol cluster **III-c1**. (b) Structure of the extracted biphenanthrol cluster **III-c2**. (c) Structure of the extracted 1D structural unit. (d) Cavity with the inclusion of guest *n*PrOH molecules observed along the *a* axis. Solid arrows show phenanthrene–phenanthrene edge-to-face interactions.

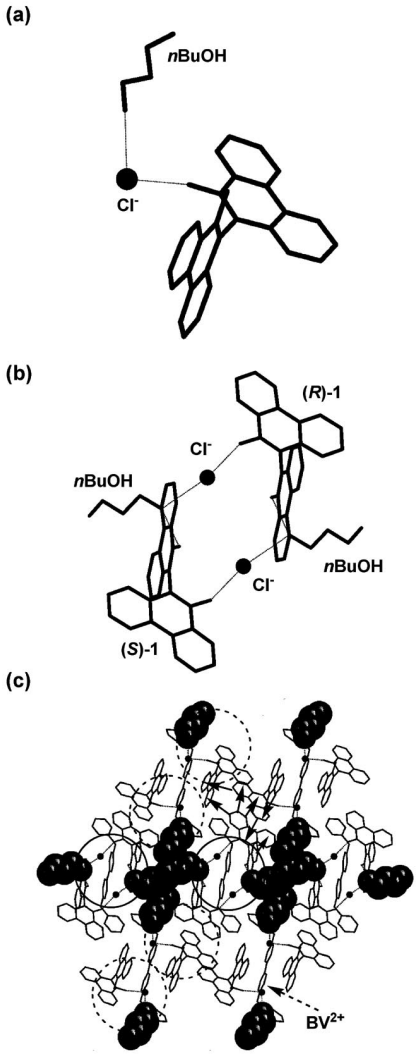

Figure 6. Structure of **IV**. (a) Structure of the extracted biphenanthrol component unit **IV-c1**. (b) Structure of the extracted biphenanthrol cluster **IV-c2**. (c) Channel-like cavity formed by the self-assembly of the biphenanthrol component unit observed along the *a* axis. Solid arrows show phenanthrene–phenanthrene edge-to-face interactions. Dotted and solid circles show **IV-c1** and **IV-c2**, respectively.

Table 2. Distances between the nearest molecule pairs in **III** and **IV**.[a]

	Distance [Å]				
	$BV^{2+}\cdots BV^{2+}$	$BV^{2+}\cdots Cl^{-}$	$BV^{2+}\cdots$**1**	**1**$\cdots Cl^{-}$	**1**$\cdots$**1**
III	4.84 (C···C)	3.65 (C···Cl)	3.23 (C···O)	3.00 (O···Cl)	3.59 (C···C)
IV	3.58 (C···C)	3.56 (C···Cl)	3.18 (C···O)	3.02 (O···Cl)	3.41 (C···C)

[a] The distance between the nearest intermolecular atom pair (non-hydrogen) is provided.

plexes are remarkably different. Although the distance between the nearest viologen cations in **II** (3.96 Å) is longer than that in **IV** (3.58 Å), the wavelength of the absorption edge of **II** (620 nm) is longer than that of **IV** (580 nm). This difference in the optical property would result from the fact that the electron affinity of MV^{2+} is significantly greater than that of BV^{2+}. Theoretical calculations suggest that the second ionization energies of MV and BV are 8.8 and 7.9 eV, respectively. The *rac*-**1**/$MVCl_2$ system, therefore, tends to yield the absorption edge at a longer wavelength than the *rac*-**1**/$BVCl_2$ system. This suggests that the absorption of this CT host system is mainly dependent on both the electron-accepting property of the viologen cation used and the effect of the distance between the nearest viologen cations. Moreover, by comparing these two host systems we observed that the guest-dependent change in the DRS of the *rac*-**1**/$BVCl_2$ system was only small. From X-ray crystallographic analyses, the difference in the distances between the nearest significant molecule pairs in **III** and **IV** was found to be smaller than that in **I** and **II**. This would imply that the separations of the host molecules (particularly of the viologen cations) in the *rac*-**1**/$BVCl_2$ system are less sensitive to the guest molecule than the separations of the host molecules in the *rac*-**1**/$MVCl_2$ system.

Conclusions

A supramolecular charge-transfer host system composed of *rac*-**1** as the electron-donor and a viologen derivative as electron-acceptor has been developed. From X-ray crystallographic analysis it was found that this CT host system can include an *n*-alkyl alcohol as the guest by changing the combination and coordination style of **1**, the chloride ion, and the water molecule that constitute the host system. The color and DRS of this inclusion CT crystal are sensitive to the structure of the included *n*-alkyl alcohol. The molecular recognition properties can be tuned by changing the viologen derivatives. Moreover, one of the factors that determine the absorption of this CT host system appears to be the electron-accepting nature of the viologen cation used and the effect of the distance between the nearest viologen cations. This further enhances the potential of this CT host system, thus enabling its application in the design of novel solid-state visual indicators for molecular recognition.

Experimental Section

Formation of a CT Crystal with Inclusion of an *n*-Alkyl Alcohol Molecule as a Guest: *rac*-**1** (10.0 mg, 2.58×10^{-2} mmol) and the desired viologen derivative (2.58×10^{-2} mmol) were dissolved in the corresponding *n*-alkyl alcohol solutions (2 mL) with heating. Each solution was allowed to stand at room temperature. After 2–7 days, the respective colored crystals [**I** from *n*PrOH and *rac*-**1**/$MVCl_2$ (9.7 mg), **II** from *n*BuOH and *rac*-**1**/$MVCl_2$ (8.7 mg), **III** from *n*PrOH and *rac*-**1**/$BVCl_2$ (10.0 mg), and **IV** from *n*BuOH and *rac*-**1**/$BVCl_2$ (9.5 mg)] were deposited and collected. The weight of each type of crystal is the total crop of the crystals obtained in a single batch.

Measurement of the DRS of the CT Crystal: The DRS of the crystals were measured by using a HITACHI U-4000 spectrometer.

X-ray Crystallographic Study: The X-ray diffraction data for single crystals were collected by using a Bruker Apex spectrometer. The crystal structures were solved by the direct method[6] and refined

by the full-matrix least-squares method by using SHELX97.[7] The structures were drawn by using PLATON.[8] Absorption corrections were performed by using SADABS.[9] The non-hydrogen atoms were refined with anisotropic displacement parameters and the hydrogen atoms were included in the models at their calculated positions in the riding-model approximation.

Crystallographic Data for I: $0.5C_{12}H_{14}Cl_2N_2{\cdot}C_{28}H_{18}O_2{\cdot}C_3H_8O{\cdot}H_2O$, M = 593.11, triclinic, space group $P\bar{1}$, a = 9.2804(8), b = 10.1749(9), c = 17.6738(16) Å, α = 80.247(2), β = 77.003(2), γ = 64.981(2)°, V = 1468.3(2) Å^3, Z = 2, D_c = 1.342 g cm^{-3}, μ(Mo-K_α) = 0.174 mm^{-1}, 13007 reflections measured, 6591 unique, final $R(F^2)$ = 0.0625 using 4517 reflections with $I > 2.0\sigma(I)$, R(all data) = 0.0979, T = 120(2) K.

Crystallographic Data for II: $0.5C_{12}H_{14}Cl_2N_2{\cdot}C_{28}H_{18}O_2{\cdot}C_4H_9O{\cdot}H_2O$, M = 607.14, triclinic, space group $P\bar{1}$, a = 9.3019(6), b = 11.4319(7), c = 15.3935(10) Å, α = 87.3230(10), β = 85.2890(10), γ = 69.6400(10)°, V = 1529.18(17) Å^3, Z = 2, D_c = 1.319 g cm^{-3}, μ(Mo-K_α) = 0.168 mm^{-1}, 13607 reflections measured, 6871 unique, final $R(F^2)$ = 0.0535 using 5563 reflections with $I > 2.0\sigma(I)$, R(all data) = 0.0661, T = 200(2) K.

Crystallographic Data for III: $C_{12}H_{14}Cl_2N_2{\cdot}2C_{28}H_{18}O_2{\cdot}4C_3H_8O$, M = 1422.56, triclinic, space group $P\bar{1}$, a = 11.1390(9), b = 13.9070(11), c = 25.324(2) Å, α = 98.0190(10), β = 90.1750(10), γ = 108.1730(10)°, V = 3686.3(5) Å^3, Z = 3, D_c = 1.282 g cm^{-3}, μ(Mo-K_α) = 0.150 mm^{-1}, 32346 reflections measured, 16503 unique, final $R(F^2)$ = 0.0723 using 11348 reflections with $I > 2.0\sigma(I)$, R(all data) = 0.1078, T = 120(2) K.

Crystallographic Data for IV: $C_{12}H_{14}Cl_2N_2{\cdot}2C_{28}H_{18}O_2{\cdot}2C_4H_9O$, M = 1330.42, triclinic, space group $P\bar{1}$, a = 9.2932(9), b = 15.1597(15), c = 24.322(2) Å, α = 100.716(2), β = 91.558(2), γ = 93.216(2)°, V = 3359.0(6) Å^3, Z = 2, D_c = 1.315 g cm^{-3}, μ(Mo-K_α) = 0.158 mm^{-1}, 19492 reflections measured, 13409 unique, final $R(F^2)$ = 0.0800 using 4657 reflections with $I > 2.0\sigma(I)$, R(all data) = 0.2082, T = 115(2) K.

CCDC-671603 (for **I**), -671604 (for **II**), -683182 (for **III**), and -683183 (for **IV**) contain the supplementary crystallographic data for this paper. These data can be obtained free of charge from The Cambridge Crystallographic Data Centre via www.ccdc.cam.ac.uk/data_request/cif.

Calculation Methods: The second ionization energies of MV and BV were calculated by density functional theory (B3LYP functional[10]) with the cc-pVDZ basis set.[11] Note that the second ionization energies (adiabatic) were calculated by using the geometries of the respective dications as the viologen molecules in the complexes assume this ionic state in the electronic ground state. The Gaussian 03 program was used for these calculations.[12]

[1] a) J. L. Atwood, J. E. D. Davies, D. D. MacNicol (Eds.), *Inclusion Compounds*, Academic Press, New York, **1984**, vol. 1–3; b) D. M. Walba, N. A. Clark, H. A. Razavi, D. S. Parmar in *Inclusion Phenomenon and Molecular Recognition* (Eds.: J. L. Atwood), Plenum Press, New York, **1990**; c) J. -M. Lehn, J. L. Atwood, J. E. D. Davies, D. D. MacNicol, F. Vogtle (Eds.), *Comprehensive Supramolecular Chemistry*, Pergamon Press, Oxford, **1996**, vols. 1–11; d) J. L. Atwood, J. W. Steed (Eds.), *Encyclopedia of Supramolecular Chemistry*, Mercel Dekker, New York, **2004**; e) F.Toda, R. Bishop (Eds.), *Perspectives in Supramolecular Chemistry*, Wiley, Chichester, **2004**, vol. 8.

[2] a) Y. Imai, T. Sato, R. Kuroda, *Chem. Commun.* **2005**, 3289–3291; b) Y. Imai, K. Kawaguchi, T. Sato, R. Kuroda, Y. Matsubara, *Tetrahedron Lett.* **2006**, *47*, 7885–7888; c) K. Kodama, Y. Kobayashi, K. Saigo, *Chem. Eur. J.* **2007**, *13*, 2144–2152; d) K. Kodama, Y. Kobayashi, K. Saigo, *Cryst. Growth Des.* **2007**, *7*, 935–939; e) Y. Imai, K. Murata, K. Kawaguchi, T. Sato, R. Kuroda, Y. Matsubara, *Org. Lett.* **2007**, *9*, 3457–3460; f) Y. Imai, K. Kawaguchi, K. Asai, T. Sato, R. Kuroda, Y. Matsubara, *CrystEngComm* **2007**, *9*, 467–470; g) Y. Mizobe, T. Hinoue, M. Miyata, I. Hisaki, Y. Hasegawa, N. Tohnai, *Bull. Chem. Soc. Jpn.* **2007**, *80*, 1162–1172; h) Y. Imai, K. Murata, K. Kawaguchi, T. Sato, N. Tajima, R. Kuroda, Y. Matsubara, *Chem. Asian J.* **2008**, *3*, 625–629, and references cited therein.

[3] a) Y. Imai, N. Tajima, T. Sato, R. Kuroda, *Chirality* **2002**, *14*, 604–609; b) Y. Imai, N. Tajima, T. Sato, R. Kuroda, *Org. Lett.* **2006**, *8*, 2941–2944; c) Y. Imai, K. Kamon, T. Kinuta, N. Tajima, T. Sato, R. Kuroda, Y. Matsubara, *Tetrahedron Lett.* **2007**, *48*, 6321–6325.

[4] Y. Imai, S. Kido, K. Kamon, T. Kinuta, N. Tajima, T. Sato, R. Kuroda, Y. Matsubara, *Org. Lett.* **2007**, *9*, 5047–5050.

[5] M. Noji, M. Nakajima, K. Koga, *Tetrahedron Lett.* **1994**, *35*, 7983–7984.

[6] G. M. Sheldrick, *SHELX97, Program for the solution of crystal structures*, University of Göttingen, Germany, **1997**.

[7] G. M. Sheldrick, *SHELX97, Program for the refinement of crystal structures*, University of Göttingen, Germany, **1997**.

[8] A. L. Spek, *PLATON, Molecular geometry and graphics program*, University of Utrecht, The Netherlands, **1999**.

[9] G. M. Sheldrick, *SADABS, Program for empirical absorption correction of area detector data*, University of Göttingen, Germany, **1996**.

[10] A. D. Becke, *J. Chem. Phys.* **1993**, *98*, 5648–5652.

[11] T. H. Dunning Jr., *J. Chem. Phys.* **1989**, *90*, 1007–1023.

[12] M. J. Frisch, G. W. Trucks, H. B. Schlegel, G. E. Scuseria, M. A. Robb, J. R. Cheeseman Jr., J. A. Montgomery, T. Vreven, K. N. Kudin, J. C. Burant, J. M. Millam, S. S. Iyengar, J. Tomasi, V. Barone, B. Mennucci, M. Cossi, G. Scalmani, N. Rega, G. A. Petersson, H. Nakatsuji, M. Hada, M. Ehara, K. Toyota, R. Fukuda, J. Hasegawa, M. Ishida, T. Nakajima, Y. Honda, O. Kitao, H. Nakai, M. Klene, X. Li, J. E. Knox, H. P. Hratchian, J. B. Cross, V. Bakken, C. Adamo, J. Jaramillo, R. Gomperts, R. E. Stratmann, O. Yazyev, A. J. Austin, R. Cammi, C. Pomelli, J. W. Ochterski, P. Y. Ayala, K. Morokuma, G. A. Voth, P. Salvador, J. J. Dannenberg, V. G. Zakrzewski, S. Dapprich, A. D. Daniels, M. C. Strain, O. Farkas, D. K. Malick, A. D. Rabuck, K. Raghavachari, J. B. Foresman, J. V. Ortiz, Q. Cui, A. G. Baboul, S. Clifford, J. Cioslowski, B. B. Stefanov, G. Liu, A. Liashenko, P. Piskorz, I. Komaromi, R. L. Martin, D. J. Fox, T. Keith, M. A. Al-Laham, C. Y. Peng, A. Nanayakkara, M. Challacombe, P. M. W. Gill, B. Johnson, W. Chen, M. W. Wong, C. Gonzalez, J. A. Pople, *Gaussian 03, Revision C.02*, Gaussian, Inc., Wallingford, CT, **2004**.

Received: June 11, 2008
Published Online: August 27, 2008

